HOKKAIDO UNIVERSITY

Title	Theory of inverse problems for crack bridging stresses determination
Author(s)	Nazmul, I. M.; Matsumoto, T.
Citation	International Journal of Solids and Structures, 49(1), 191-196 https://doi.org/10.1016/j.ijsolstr.2011.09.023
Issue Date	2012-01
Doc URL	https://hdl.handle.net/2115/47986
Type	journal article
File Information	IJSS49-1_191-196.pdf

Hokkaido University Collection of Scholarly and Academic Papers : HUSCAP

THEORY OF INVERSE PROBLEMS FOR CRACK BRIDGING STRESSES DETERMINATION

By I. M. Nazmul[1] and T. Matsumoto[2]

[1]Associate Professor, Department of Civil Engineering, Presidency University, Plot 11A, Gulshan 2, Dhaka 1212, Bangladesh. E mail: islammn@presidency.edu.bd. Phone: +88028857617 (ext. 501). Fax: 88028831184.

[2]Associate Professor, Division of Built Environment , Graduate School of Engineering, Hokkaido University, Kita 13, Nishi 8, Kita-ku, Sapporo 060-8628, Japan, Phone: +81-11-706-6171, Fax: +81117066172, E mail: takashim@eng.hokudai.ac.jp

Abstract: A new mathematical procedure has been proposed for the determination of crack bridging stresses from perturbed Crack Opening Displacements (COD) in fiber composites. The problem is an ill-posed inverse problem and the proposed procedure exploited concepts from Functional Analysis and the Theory of Inverse Problems. The transformation from crack bridging stress into COD has been linearized, where the continuous crack bridging stresses functions of infinite dimensional vector spaces were approximated into finite dimensional subspaces. The coordinate representation of functions and the matrix of the transformation facilitated a numerical solution to the inverse problem. Self consistent direct and inverse problems were solved numerically in context to an example. Results establish that the proposed mathematical procedure produces fairly accurate results for engineering application.

Keywords: *crack opening displacements, coordinate representation of vectors, matrix of a transformation, inverse problem, crack bridging stresses.*

1. Introduction

The relation between crack bridging stresses and COD is termed as the bridging law of a fiber composite and is a material property. Determination of the bridging law for a fiber composite, either theoretically or experimentally is fundamental for its engineering application. Primary theoretical assumptions on the fiber bridging characteristics and the fundamental analytical models are available in the pioneering works by Aveston *et al*. [1971], Marshall *et al*. [1985] and Budiansky *et al*. [1986].

Practical calibrations of the bridging law were performed by a J-based-fracture-testing method [Li *et al*. (1994)] and by simultaneous COD and fiber stress/strain measurements [Carman and Sendeckyi (1995) and Studer *et al.* (2002)]. Theoretically, crack bridging stresses were computed by the evaluation of the R-curve [Fett *et al.* (1996)], by compliance analysis [Ebrahimi *et al.* (2003)] and by finite element method [Buchanan *et al*. (1997)].

Theoretical evaluation of crack bridging stresses from perturbed COD data was accomplished by Cox and Marshall [1991a] on the analytical models of Cox and Marshall [1991b]. The evaluation consisted of inverse analysis by the Tikhonov regularization method. Those direct and inverse computations were further extended by Massabo and Cox [1999] and Massabo *et al*. [1998].

The mathematical procedure for the determination of crack bridging stresses from perturbed COD data proposed in this paper also stems from the analytical models of Cox and Marshall [1991b]. The contributions of the current mathematical procedure include approximation of the bridging stress function in a finite dimensional subspace, coordinate representation of the interpolated COD profile function in terms of an orthogonal basis set, determination of the numerical equivalent (the matrix) of the transformation between crack bridging stress and COD and derivation of the normal equation from the Tikhonov functional within finite dimensional linear spaces.

2. The Linear Transformation

The proposed mathematical procedure of estimating crack bridging stresses from perturbed COD originated in the analytical model proposed by Cox and Marshall [1991b]. The model relates crack bridging stresses $p\{u(x)\}$ with COD $u(x)$ by the following integral equation

$$u(x) = \frac{4}{E'} \int_x^a \left\{ \int_0^{a'} G(x', a', w)[\sigma_a(x') - p\{u(x')\}]dx' G(x, a', w)da' \right\} \tag{1}$$

where a is the crack length, w is the specimen dimension (e.g. width), $\sigma_a(x')$ is the stress that would exist on the crack surface in absence of cracking, E' is a combination of elastic constants depending on stress state (plane stress/plane strain) and material isotropy, and $G(x, a, w)$ is a weight function of the crack geometry. Standard forms of $G(x, a, w)$ for a large number of crack geometries are available in the handbooks of stress intensity factors [e.g. Tada *et al.* (1985)].

The direct problem of Eq. (1) is to determine COD $u(x)$, for a given crack geometry, external load and material. But before that, either a bridging stress – COD relation $p(u)$, or a bridging stress – distance relation $p(x)$, is to be known, assumed or evaluated by tests.

The inverse problem Eq. (1) would evaluate either $p(u)$ or $p(x)$ from given COD $u(x)$ for a given geometry and external load. Theoretical and unperturbed COD data would result in a unique theoretical bridging law, which would continuously depend on the data. But real COD data supposedly contain observational errors. A small perturbation in the data might generate large errors in the results of the inverse problem of Eq. (1), which is constituted by integrations. Thus the inverse problem would be ill-posed. A proper regularization procedure is required to yield a sufficiently accurate solution for engineering purposes.

In order to obtain a linear transformation from the integral transform of Eq. (1), the estimated COD $u(x)$ is thought to be composed of two effects. First, cracks are opened due to the external load $\sigma_a(x')$ with the profile $u_a(x)$, and second, crack bridging stresses close the crack by $u_b(x)$ [Cox and Marshall (1991b)]. So,

$$u(x) = u_a(x) - u_b(x). \tag{2}$$

The direct problem of deducing $u_a(x)$ is deterministic for a given crack geometry, external load and material. The solution given by

$$u_a(x) = \frac{4}{E'} \int_x^a \left[\int_0^{a'} G(x', a', w)\sigma_a(x')dx' \right] G(x, a', w)da', \tag{3}$$

does exist, is unique and continuously depend on the input data. Thus the direct problem of Eq. (3) is well-posed. Likewise, the direct problem of evaluation of crack closing due to crack bridging stresses given by

$$u_b(x) = \frac{4}{E'} \int_x^a \left[\int_0^{a'} G(x', a', w)p\{u(x')\}dx' \right] G(x, a', w)da', \tag{4}$$

would also be well-posed, if the bridging law $p\{u(x')\}$ had been constituted beforehand. However, the inverse problem of deducing $p\{u(x)\}$ from $u_b(x)$ is stochastic and ill-posed (regularizable or non-regularizable) based on the level of perturbation of the input COD.

The regularization procedure proposed in this paper is relevant to the transformation of Eq. (4). This is a product transformation of two Volterra integral equations of the first kind, namely

$$T_1 := \int_0^{a'} G(x', a', w)p\{u(x')\}dx' = v(a') \tag{5}$$

$$T_2 := \int_x^a G(x, a', w)v(a')da' = u_b(x) \tag{6}$$

where $T_1 : W \to V$ and $T_2 : V \to U$ for $p \in W$, $v \in V$ and $u_b \in U$. The product transformation $T = T_2 T_1 : W \to U$ is defined to transform crack bridging stresses $p\{u(x)\}$ into crack closings $u_b(x)$ as

$$Tp = u_b \tag{7}$$

The Volterra transformations and their product mappings are linear [Michael and Herget (1985)]. It is assumed that the linear spaces W, V, $U \subset C(0, a)$, where $C(0, a)$ is the Hilbert space of real-valued continuous functions within $(0, a)$.

All variables are normalized for further calculations and Eqs. (1), (3) and (4) have been deduced in their normalized forms. The definitions of normalized COD *U*, normalized external load *S*, normalized crack bridging stresses *P* and normalized crack length *C* are given by [Cox and Marshall (1991a)]

$$U = u \Big/ \frac{4\pi E_f E}{\Sigma^2 R(1-f)E_m} \tag{8}$$

$$S = \frac{\sigma}{f\Sigma} \tag{9}$$

$$P = \frac{p}{f\Sigma} \tag{10}$$

$$C = a \Big/ \frac{\pi\sigma R(1-f)E_m}{16\pi f E_f (1-\nu^2)} \tag{11}$$

3. Finite Dimensional Approximations of the Bridging Stress Function

Although the dimension of a function space is generally infinite, the continuous functions of $C(0, a)$ may be approximated within finite dimensional subspaces. This approximation error is generally negligible for large dimensions and must be checked. In this paper, the vectors (functions) of the infinite dimensional spaces *W*, *V* and *U* are approximated to be contained within *l*, *m* and *n* dimensional linear subspaces, spanned by the basis sets $\{e_1, \ldots\ldots, e_l\} \in W$, $\{f_1, \ldots\ldots, f_m\} \in V$ and $\{g_1, \ldots\ldots, g_n\} \in U$ respectively.

To check this approximation, first, the well accredited bridging stress function [Cox and Marshall (1991a)] has been reduced to correspond to a certain continuously aligned fiber composite whose fiber strengths distribution falls into a Weibull distribution of modulus 2 as

$$P(U) = \sqrt{U}\, e^{-U^{1.5}}. \tag{12}$$

Next, the function of Eq. (12) is approximated within the subspace *W* by the coordinates $\{\varepsilon_1, \ldots\ldots, \varepsilon_m\}$ as

$$P'(U) = \varepsilon_1 e_1 + \ldots\ldots + \varepsilon_l e_l, \tag{13}$$

where $P(U)$ and $P'(U)$ are the exact and approximated bridging stress functions respectively. Fig. 1 demonstrates this finite dimensional approximation considering several trial dimensions of the subspace *W*, where ChebyShev polynomials of the second kind have been used as the basis set $\{e_1, \ldots\ldots, e_l\}$. It is observed that better convergence is attained for higher values of *l*, and the error becomes very insignificant for $l \geq 5$.

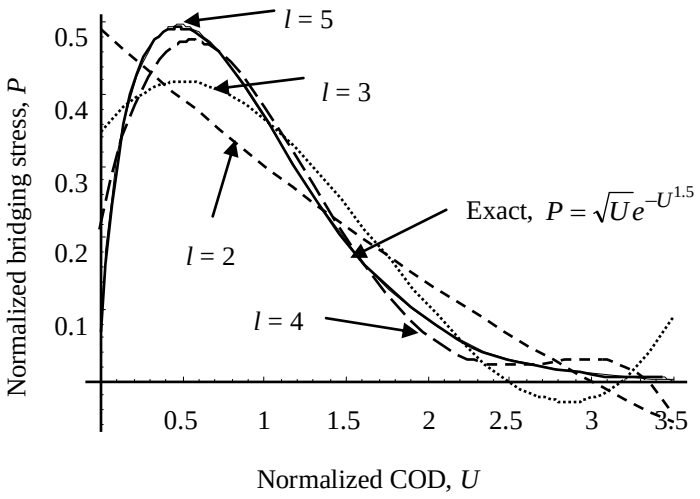


Fig. 1. A graphical demonstration of finite dimensional approximation relevant to bridging stress function of fiber composites.

4. Coordinate Representation of COD Data

The input data into the inverse problem are the COD values. COD data should be collected at a grid of points along the crack; from the crack mouth to the crack tip. The grid points could be equally or unequally spaced, nevertheless, an unequal grid having closely spaced points near the crack tip is suggested as COD values vary very fast at these locations. A grid of points located by a sine function is helpful [Cox and Marshall (1991a)]

$$x := \left\{ x_r, x_r = a \sin \frac{r\pi}{2q} \text{ for } r = 1,.....q \right\}. \tag{14}$$

The measured COD values at the grid points are

$$u := \{u_r, r = 1,.....q\}. \tag{15}$$

The crack openings due to external load $u_a(x)$ at the grid points are computed by Eq. (3) as

$$u_a := \{u_{ar}, r = 1,.....q\} \ . \tag{16}$$

The crack closings due to the bridging stresses at the grid points to be determined by Eq. (4) would also be computed by Eq. (2) as

$$u_b := u_{br} = \{u_{ar} - u_r, \ r = 1,.....q\}. \tag{17}$$

The trend line of the data set (u_{br}, x_r) is approximated by the function $u_b(x)$. The function, in turn, is spanned by a linear combination of scalars and base vectors of finite dimension. This is the coordinate representation of a function with respect to the basis; the scalars being called the coordinates. Linear regression analyses are followed to obtain the function $u_b(x)$ with respect to the basis $\{g_1,.....,g_n\} \in U$ as

$$u_b(x) = \beta_1 g_1 + \beta_2 g_2 + ...+ \beta_n g_n + E \tag{18}$$

where E is the statistical error. The coordinates $\{\beta_1,.....,\beta_n\}$ are the solution to the linear system obtained by minimizing the error E as

$$\sum_r E_r{}^2 = \sum_r [u_{br} - (\beta_1 g_1 + ...+ \beta_n g_n)]^2 \ . \tag{19}$$

The approximation is checked graphically in Fig. 2, where Legendre and Chebyshev polynomials of the first kind (ChebyshevT) yielded perfect fits of $u_b(x)$ with the data. The approximation is mathematically checked by

$$\|u_b - u_b(x)\| \le \varepsilon, \tag{20}$$

where $\|\varepsilon\| \to 0$.

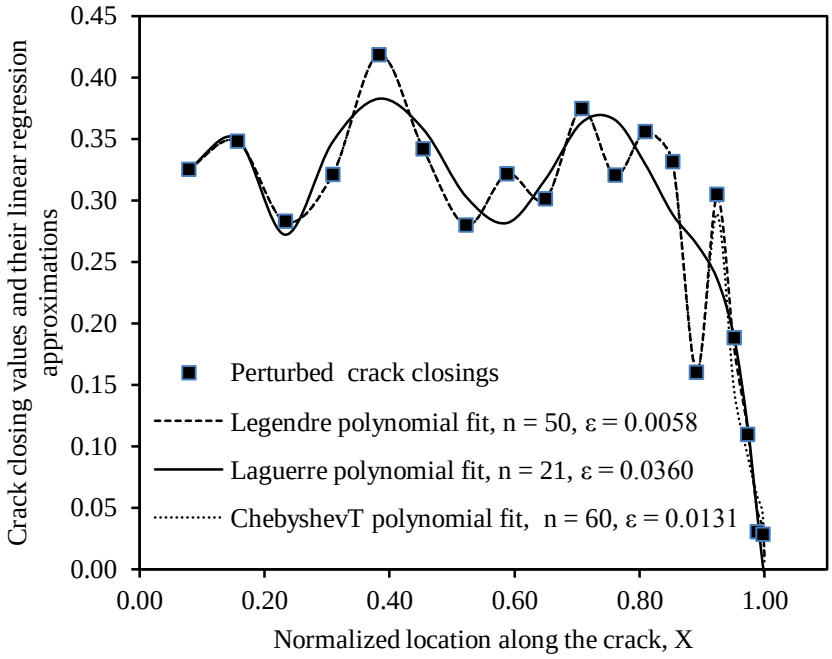


Fig. 2. Approximations of u_b by several orthogonal base vectors

Similar regression analyses would yield coordinate representation of $v(x)$, relevant to data sets (v_r, x_r). Thus the functions $u_b(x)$, $v(x)$ and $p(x)$ are expressed in terms of their coordinate representations as

$$u_b := \mathbf{u_b}^{\mathbf{T}} = \{\beta_1, \ldots\ldots, \beta_n\} \tag{21}$$

$$v := \mathbf{v}^{\mathbf{T}} = \{\gamma_1, \ldots\ldots, \gamma_m\} \tag{22}$$

$$p := \mathbf{p}^{\mathbf{T}} = \{\varepsilon_1, \ldots\ldots, \varepsilon_l\} \tag{23}$$

where the superscript T means transpose.

Convergence is tested in all regression analyses and the best fit is chosen. Legendre polynomials were found superior for the spaces *U* and *V* and Chebyshev polynomials of the first kind were used for *W*.

5. Matrix of the Transformation

This section approximates the transformations T_1 and T_2 (Eqs. (5, 6)) by their matrices $\mathbf{T_1}$ and $\mathbf{T_2}$ respectively. The entries of the matrices $\mathbf{T_1}$ and $\mathbf{T_2}$ are computed by applying the relevant transformations to the base vectors of the domain of the transformation as [Michael and Herget (1985)]

$$T_1 e_i = e_i' = \sum_{j=1}^{m} t_{ij}^1 f_j \quad \text{for } i = 1, \ldots\ldots, l \tag{24}$$

$$T_2 f_j = f_j' = \sum_{k=1}^{n} t_{jk}^2 g_k \quad \text{for } j = 1, \ldots\ldots, m \tag{25}$$

where $t_{ij}^1 \in \mathbf{T}_1$ and $t_{jk}^2 \in \mathbf{T}_2$. The product $\mathbf{T}$ of the conformal matrices $\mathbf{T_1}$ and $\mathbf{T_2}$ represents the product transformation *T* as

$$\mathbf{T} = \mathbf{T_1}\mathbf{T_2} \ . \tag{26}$$

The entries of **T** are

$$t_{ik} = \sum_{j=1}^{m} t_{ij}^{1} t_{jk}^{2} \in \mathbf{T} \text{ for } i = 1,.....l \text{ and } k = 1,.....n \tag{27}$$

6. Ill-posedness of the Inverse Transformation

The solution to Eq. (7) is given by

$$p = T^{-1} u_b; \text{ for } u_b \in U, \text{ and } p \in W . \tag{28}$$

The theoretical crack bridging stresses, $p \in \mathcal{D}(T)$ would be obtained from the theoretical and unperturbed data $u_b \in \mathcal{R}(T)$, $\mathcal{D}(T)$ and $\mathcal{R}(T)$ being the domain and the range of the transformation *T*. If the transformation *T* was compact and one-to-one, the inverse transformation T^{-1} would exist and the solution would be unique.

But real data are perturbed compared to the theoretical predictions due to the observational errors and the underlying assumptions in hypothetical modeling. Therefore, instead of a theoretical list $\{u\}$ predicted in Eq. (15), a perturbed list of data $\{u^{\delta}\}$ with an error level $\|\delta\| > 0$ is obtained as

$$u^{\delta} := \{u_r^{\delta}, r = 1,.....q\} \tag{29}$$

As a consequence, data in Eq. (17) are perturbed as

$$u_b^{\delta} := \{u_{br}^{\delta}, r = 1,.....q\} \tag{30}$$

The level of perturbation defined as

$$\|u_{br} - u_{br}^{\delta}\| \le \delta \tag{31}$$

is helpful to the determination of the regularization parameter [Tikhonov *et. al*. (1990)].

Thus Eq. (7) is perturbed with perturbed data as

$$Tp^{\delta} = u_b^{\delta} . \tag{32}$$

Generally speaking, $u_b^{\delta} \notin \mathcal{R}(T)$ and a unique solution (or even a solution) of Eq. (32) might not exist. Even if it exists, it might not depend continuously on the real data, and in case of the worst-case error, a small perturbation in data might lead to large variations in results (Kirsch 1996). Thus the problem is improperly posed or ill-posed and warrants for a regularization strategy.

The objective of the regularization strategy is to construct a bounded linear approximation of the inverse transformation. An approximate solution is sought as

$$p^{\delta} = T_h^{-1} u_b^{\delta}; \text{ for } u_b^{\delta} \in U, \text{ and } p^{\delta} \in W \tag{33}$$

The approximation in the transformation, namely T_h instead of *T* in Eq. (33) primarily originates from determination of the matrix of the transformation, but further approximations are inevitable based on the choice of the regularization parameter.

7. Solution by the Tikhonov Functional

The Tikhonov functional is [Tikhonov *et al*. (1990)]

$$M^{\alpha}[p] = \|T_{h,\alpha}\, p - u_b^{\delta}\|_U^2 + \alpha \|p\|_W^2 , \tag{34}$$

$\alpha > 0$ being the regularization parameter. The approximation in the transformation is measured as

$$\|T_{h,\alpha} - T\| \le h , \tag{35}$$

for $h \to 0$. A family of regularization strategies may be formulated depending on α , giving rise to a family of transformations $T_{h,\alpha}^{-1} : U \to W$ for which

$$\lim_{\alpha \to 0} T_{h,\alpha}^{-1} T\, p^{\delta} \approx p\,. \tag{36}$$

The regularization parameter α depends on the values of *h* and δ discussed in Eq. (31) and Eq. (35) respectively. The minimization of the functional stated in Eq. (34) is converted into the solution to a normal equation admissible by the following theorem [Kirsch (1996)].

Theorem 7.1: Let $T : W \to U$ be a linear and bounded operator between Hilbert spaces and $\alpha > 0$. Then the Tikhonov functional $M^{\alpha}[p]$ has a unique minimum $p^{\alpha} \in W$. This minimum is the unique solution to the following normal equation

$$\alpha\, p^{\alpha} + T^{*} T\, p^{\alpha} = T^{*} u \tag{37}$$

where T* is the adjoint of T.

Adjoint operators in matrix representations are easily determined by the transpose. It is seen from Eq. (37) that the inverse approximate operator is obtained depending on α as

$$T_{h,\alpha}^{-1} := \left(\alpha I + T_{h,\alpha}^{*} T_{h,\alpha}\right)^{-1} T_{h,\alpha}^{*} : U \to W \tag{38}$$

and a family of solutions p^{δ} can be found by

$$p^{\delta} = T_{h,\alpha}^{-1} u_b\,. \tag{39}$$

In case of perturbed data, this regularization strategy is further supported by the following theorem [Kirsch (1996)]

Theorem 7.2: Let $T : W \to U$ be a linear, compact operator and $\alpha > 0$. Then the operator $\alpha I + T_{h,\alpha}^{*} T_{h,\alpha}$ is boundedly invertible. The operators $T_{h,\alpha}^{-1} := \left(\alpha I + T_{h,\alpha}^{*} T_{h,\alpha}\right)^{-1} T_{h,\alpha}^{*} : U \to W$ form a regularization strategy with $\left\| T_{h,\alpha}^{-1} \right\| \le 1/2\sqrt{\alpha}$. It is called the Tikhonov regularization method. $T_{h,\alpha}^{-1} u_b^{\delta}$ is determined as the unique solution $p^{\alpha,\delta} \in W$ of the equation of the second kind

$$\alpha\, p^{\alpha,\delta} + T_{h,\alpha}^{*} T_{h,\alpha}\, p^{\alpha,\delta} = T_{h,\alpha}^{*} u_b^{\delta} \tag{40}$$

At this stage, the following matrix equation is needed to be solved

$$\mathbf{p} = \mathbf{B} \cdot \mathbf{u_b} \tag{41}$$

where **p** and $\mathbf{u_b}$ are defined in Eqs. (21) and (23), and the matrix **B** is given by

$$\mathbf{B} = \left(\alpha \mathbf{I} + \mathbf{T^T T}\right)^{-1} \cdot \mathbf{T^T} \tag{42}$$

where **I** is the identity matrix.

8. An Example

This section presents a set of self-consistent direct and inverse problems solution to a single edge notched fracture specimen while under a uniform remote loading $\sigma(x)$, as shown in Figure 3a. The weight function for this geometry given by Cox and Marshall (1991b) and Tada *et al.* (1985) is

$$G(x,a,w) = \frac{1}{\sqrt{\pi a}} \frac{s(x/a, a/w)}{\left(1 - x^2/a^2\right)^{1/2} (1 - a/w)^{3/2}} \tag{43}$$

where $s(x/a, a/w) = s(x/a, \xi)$ is given by

$$s(x/a,\xi)=s_1(\xi)+\frac{x}{a}s_2(\xi)+\frac{x^2}{a^2}s_3(\xi)+\frac{x^3}{a^3}s_4(\xi) \tag{44}$$

$$s_1(\xi)=0.46+3.06\xi+0.84(1-\xi)^5+0.66\xi^2(1-\xi)^2 \tag{45}$$

$$s_2(\xi)=-3.52\xi^2 \tag{46}$$

$$s_3(\xi)=6.17-28.22\xi+34.54\xi^2-14.39\xi^3-(1-\xi)^{3/2} -5.88(1-\xi)^5-2.64\xi^2(1-\xi)^2 \tag{47}$$

$$s_4(\xi)=-6.63+25.16\xi-31.04\xi^2+14.41\xi^3+2(1-\xi)^{3/2} +5.04(1-\xi)^5+1.98\xi^2(1-\xi)^2 \tag{48}$$

A direct solution to Eq. (1) involving numerical integration on a finely discretized grid for the crack geometry shown in Fig. 3a yields the COD profile shown as solid lines in Fig. 3b. The solution procedure requires a bridging law function, assumed in Eq. (12) and graphed in Fig. 1, which entails a predetermined COD profile. The difficulty is overcome by an iterative procedure. First, a tentative COD profile is obtained by following Eq. (3), and second Eq. (12) is applied to get a relevant bridging law. This bridging law is used in Eq. (1) to evaluate a more accurate COD profile. Consistent theoretical COD profiles shown in Fig. 3b are obtained after several iterations that fit exactly to Eq. (1) and Eq. (12).

To simulate a set of perturbed COD data, first, a set of random numbers having a normal distribution with zero mean and a certain standard deviation, μ, has been generated as

$$\delta_\mu := \{\delta_{\mu r}, r=1,.....q\} \tag{49}$$

These random numbers are added to the theoretical COD values (u_r) to make them perturbed shown by the diamond markers and dotted lines in Fig. 3b.

$$u^\delta := \{u_r^\delta = u_r+\delta_{\mu r}, r=1,.....q\} \tag{50}$$

The error level, δ, is independent of the number of grid points as it is defined in terms of a Euclidean metric suggested by Eq. (31) as

$$\delta := \frac{1}{q}\sqrt{\left\{\sum_{r=1}^{q}\left(u_r-u_r^\delta\right)^2\right\}} \tag{51}$$

Given a crack geometry and loading, the inverse problem with the set of perturbed COD should work out an approximated bridging stress function of Eq. (12) and Fig. 1, which has been entered into the direct problem.

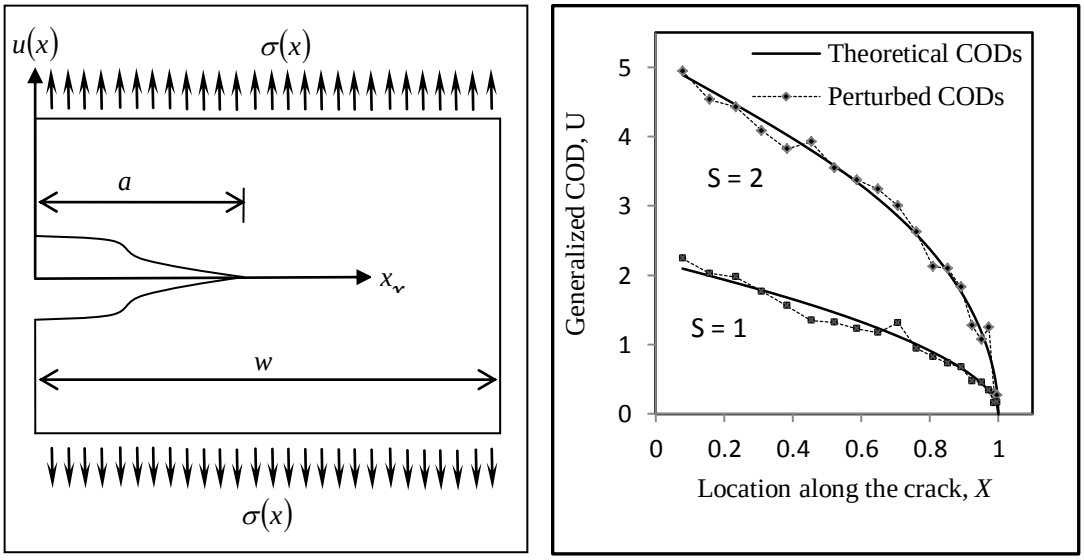


Fig. 3. Single edge notched specimen (a) geometry with uniform external load, (b) COD profiles.

Data points from the perturbed COD of Fig. 3b are entered into the inverse problem along with the crack geometry of Fig. 3a. Eq. (41) is solved for the vector **p** with the vector $\mathbf{u_b}$ from Eq. (21) formed by the perturbed u_b^{δ}. The matrix **B** is obtained by Eq. (42) with **T** matrix defined in Eq. (27), again using the perturbed transformation $T_{h,\alpha}$. Values of $\alpha > 0$ are determined by the generalized discrepancy principle [Tikhonov *et al*. (1990)] and checked by trial. Solutions to the inverse problem are shown in Fig. 4.

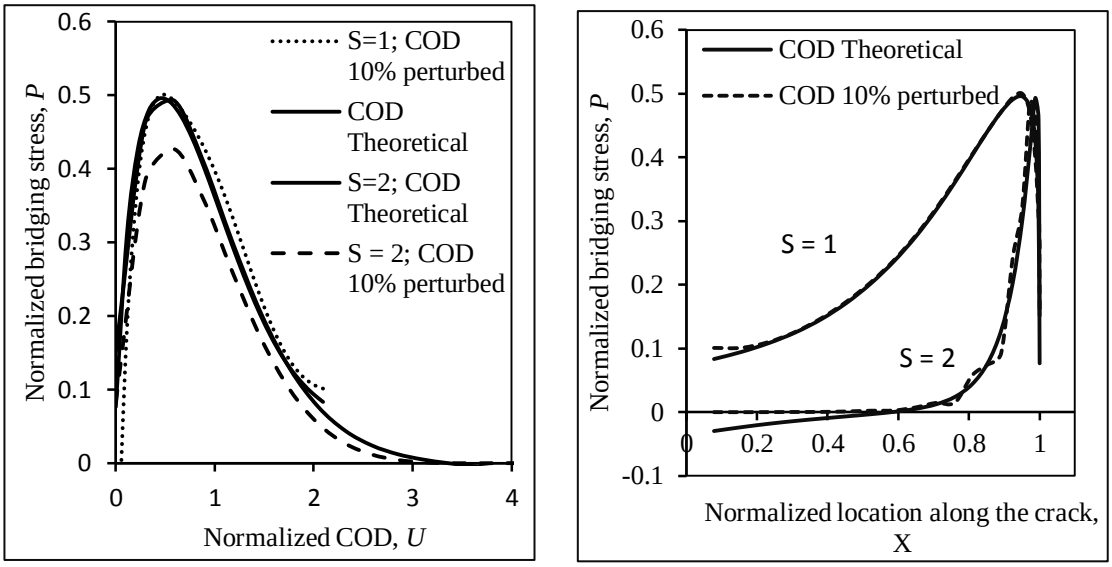


Fig. 4. Crack bridging stresses obtained by inverse problem solution, (a) bridging stress as a function of the COD, (b) bridging stress as a function of the location along the crack.

Fig. 4a shows the bridging law retrieved from the inverse problem. A quick comparison with Fig. 1 demonstrates the effectiveness and accuracy of the mathematical procedure proposed in this paper. It is observed that despite all the approximations in numerical procedures (linearization of the transformation, coordinate representations of vectors, transformation converted into matrix) the theoretical COD as well as COD with 10% perturbation retrieved the bridging law with sufficient accuracy. A more refined grid, particularly near the crack tip would be required for a better convergence in case of S = 2, where bridging stresses are concentrated very near to the crack tip, as is evident from Fig. 4b.

A data-set having more than 10% perturbation works out a more approximate solution. However, recent measuring techniques of image analysis, scanning electron microscope, laser interferrometric displacement gauge are able to assess COD up to 5% errors. Any regularization strategy must be applied with knowledge of the error level in data collection as has been successfully demonstrated with real data by Nazmul and Matsumoto (2008) and Massabo *et al*. (1998).

9. Conclusion

A mathematical procedure based on the theory of inverse problems and functional analysis has been established to determine crack bridging stresses from COD in fiber composites. All functions are approximated by coordinate representation within finite dimensional basis sets. The transformation between the crack bridging stresses and the COD is also approximated numerically by its matrix. The Tikhonov method of regularization has been applied to solve the ill-posed inverse problem in case of perturbed COD data. An example demonstrated the pertinence of the proposed mathematical procedure.

10. References

Aveston, J. Cooper, G. A. and Kelly, A. (1971). The properties of fibre composites. Conference Proceedings, *National Physics Laboratory, Guildford, IPC Science And Technology Press Ltd.* pp. 15 - 26.

Belnap, J. D. and Shetty, D. K. (1998). Micromechanics of crack bridging in sapphire/epoxy composites, *Compos. Sci. Technol.* **58**: 11, pp. 1763-1773.

Buchanan, D. J., John, R. and Johnson, D. A. (1997). Determination of crack bridging stress from crack opening displacement profiles, *Int. J. Fracture,* **87**: 2, pp. 101-117.

Budiansky, B., Hutchinson, J. W. and Evans, A. G. (1986). Matrix fracture in fiber reinforced ceramics, *J. Mech. Phys. Solids,* **34**: 2, pp. 167 – 189.

Carman, G. P. and Sendeckyj, G. P. (1995). Review of the Mechanics of Embedded Optical Sensors, *J. Compos. Tech. Res.,* **17**: 3, pp. 183 – 193.

Cox, B. N. and Marshall, D. B. (1991a). The determination of crack bridging forces, *Int. J. Fracture,* **49**: 3, pp. 159-176.

Cox, B. N. and Marshall, D. B. (1991b). Stable and unstable solutions for bridged crack in various specimens, *Acta Metall. Mater.* **39**: 4, pp. 579-589.

Ebrahimi, M.E., Chevalier, J. and Fantozzi G. (2003). R-curve evaluation and bridging stress determination in alumina by compliance analysis. *J. Eur. Ceram. Soc.* **23**: pp. 943 – 949.

Fett, T., *et al.* (1996). Correlation between long and short crack R-curves in Alumina using crack opening displacement and fracture mechanical weight function method, *J. Am. Ceram. Soc.,* **79**: 5, pp. 1189-1196.

Fett, T., *et al.* (2000). White, Bridging stress determination by evaluation of the R-curve, *J. Eur. Ceram. Soc.,* **20**: 12, pp. 2143-2148.

Kirsch, A. (1996). *An introduction to the mathematical theory of inverse problems*. Springer-Verlag, Inc., New York.

Li, V. C., Maleej, M. and Hashida, T. (1994). Experimental determination of the stress-crack opening relation in fiber cementitious composites with a crack-tip singularity. *J Mater. Sci.* **29:** pp. 2719 – 2724.

Marshall, D. B., Cox, B. N. and Evans, A. G. (1985). The mechanics of matrix cracking in brittle-matrix composites, *Acta Mater.* **33**: 11, pp. 2013-2021.

Massabo, R. and Cox, B. N. (1999). Concepts for bridged Mode II delamination cracks. *J. Mech. Phys. Solids,* **47**: 6, pp. 1265 – 1300.

Massabo, R., Mumm D. R. and Cox, B. N. (1998). Characterizing mode II delamination cracks in stitched composites. *Int. J. Fracture,* **92**: 1, pp. 1 – 38.

Michael, A. N. and Herget, C. J. (1981). *Applied algebra and functional analysis*. Dover Publications, Inc., New York.

Nazmul, I. M. and Matsumoto, T. (2008). High resolution COD image analysis for health monitoring of reinforced concrete structures through inverse analysis. *Int. J. Solids. Struct.*, **45**; 1, pp. 159 – 174.

Schutter, G. D. (2002). Advanced monitoring of cracked structures using video microscope and automated image analysis. *NDT&E Int.* **35**: 4, pp. 209-212.

Studer, M., *et al.* (2002). Studies on bridging tractions- simultaneous bridging tractions and COD measurements, *Int. J. Fracture,* **114**: 379 – 399.

Tada, H., Paris, P. C. and Irwin, G. R. (1985). *The stress analysis of cracks handbook*. Paris Productions Inc., St. Louis, Missouri.

Tikhonov, A. N., *et al.* (1990). *Numerical methods for the solutions of ill-posed problems*, Kluwer academic publishers group, Dordrecht, The Netherlands.